Syracuse University

SURFACE

Spring 5-2016

Using Simple Self-Assembling Peptides to Attain Novel Protein-Like Functions

Tyler Smith

Using Simple Self-Assembling Peptides to Attain Novel Protein-Like Functions

A Capstone Project Submitted in Partial Fulfillment of the
Requirements of the Renée Crown University Honors Program at
Syracuse University

Tyler Alan Smith

Candidate for Bachelor of Science
and Renée Crown University Honors
May 2016

Honors Capstone Project in Biochemistry

Capstone Project Advisor: _____
            Dr. Ivan V. Korendovych,
            Assistant Professor of
            Chemistry

Capstone Project Reader: _____
            Dr. Robert P. Doyle,
            Professor of Chemistry

Honors Director: _____
            Stephen Kuusisto, Director

Abstract

    Proteins carry out many extremely efficient functions, including catalysis and biomolecule recognition. Underlying this efficiency is their extraordinary complexity and ability to fold into unique three-dimensional structures. Attempts to replicate this efficiency through *de novo* design have only shown moderate success, and it is unclear how modern-day proteins may have evolved. However, short peptides that alternate hydrophobic and hydrophilic residues can self-assemble into amyloid fibrils to achieve well-defined secondary structure. These aggregates may have served as a template from which the first proteins were derived. We designed self-assembling seven-residue peptides that are able to act as Zn^{2+}-dependent esterases. Zn^{2+} acts to both help induce fibril formation and to serve as a metal cofactor to catalyze acyl ester hydrolysis. Furthermore, we developed a second set of peptides to recognize a target molecule with moderate specificity. The ability of this simple system to catalyze a chemical reaction and exhibit biomolecule recognition suggests that similar peptide aggregates may have been evolutionary precursors to modern-day proteins. Additionally, the ability to use a minimalistic design approach to generate functional fibrils could have implications for the development of simple nanostructured biomaterials. By using an alternating hydrophobic/hydrophilic template, novel functionality can be introduced into simple peptide aggregates.

Executive Summary

Proteins are the main molecular machinery inside of cells. They carry out a wide diversity of jobs, from DNA replication to recognizing foreign pathogens. Proteins are long chains, called polypeptides, of building blocks known as amino acids. Humans have 20 naturally occurring amino acids. These amino acids share a common structure, however each one differs in its "side group" (Figure ES1).
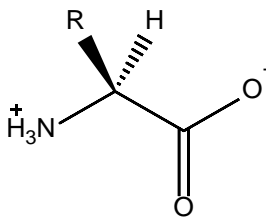
Figure ES1. The structure of an L-amino acid, found in humans. The R group can be any one of the 20 found in the naturally occurring amino acids.

This side group differs for each of the 20 naturally occurring amino acids, and covers a wide range of possible properties. Polar vs. non-polar, acidic vs. basic, and small vs. bulky are all characteristics that vary between the possible side chains. It is this variability that gives the proteins their function.

Protein chains typically fold into stable 3-dimensional structures. It is these stable conformations that allows the side groups of amino acids to be positioned such that they can reliably carry out a specific function. Antibodies, for instance, use highly specific binding interactions to recognize a target molecule, often able to differentiate between differences in a single bond at the binding site. Enzymes can not only display this specificity as well, but carry out catalysis on the bound target. Because of their high efficiency, the design of new proteins for a novel desired function has long been a "Holy Grail" of biochemistry. Being able to replicate a protein's efficiency ourselves would allow us to design new proteins for any reaction or function we want, such as the degradation of a harmful environmental contaminant.

Unfortunately, attempts to carry out this *de novo* design have only shown moderate success, and we are still unable to rival the extraordinary efficiency of proteins found in nature. New approaches are required to achieve efficient design of novel functionality.

We can gain valuable insights into new minimalistic design techniques by observing how life's first proteins evolved. A typical protein chain consists of at least 100 amino acid residues. This length produces virtually infinite numbers of possible permutations, and it is uncertain how nature could effectively test such massive numbers of possibilities randomly. However, much shorter peptides can also possess well-defined conformations through the formation of amyloid fibrils. These fibrils are composed of many individual short peptides that associate with one another to form a large, stable, plaque, similar to those found in Alzheimer's disease. One hypothesis regarding protein evolution states that the first proteins arose from similar simple amyloid-forming peptides. These peptides could organize into well-defined secondary structures capable of protein-like functions.

Using minimalistic techniques, we designed simple seven residue peptides capable of self-assembling and carrying out protein-like functions. These peptides self-assemble into large, stable, fibril structures. We designed to series of such peptides. The first series was designed to bind zinc metal ions (Figure ES2). These fibrils utilize zinc to carry out a reaction known as ester hydrolysis. Furthermore, upon mixing peptides of different sequences, synergistic activity was observed, forming fibrils of increased catalytic efficiency. The ability to mix various
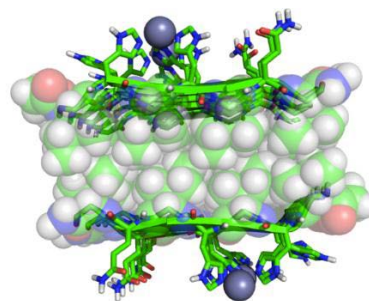

Figure ES2.

Self-assembling aggregates can be engineered to carry out enzyme-like catalysis.

peptides into a single fibril provides virtually limitless possibilities for the arrangement and structure of functional sites.

The second series of peptides were designed to specifically recognize and bind to melittin, a polypeptide found in bee venom. While high specificity is not yet achieved, we have designed the first generation of melittin-binding peptides. We expect to be able to utilize peptide-mixing strategies to enhance the specificity of the fibrils for the target molecule.

These short self-assembling functional peptides are the first of their kind. Enzyme-like catalysis from such a simple seven-residue system is unprecedented and provides a powerful platform from which more elaborate and advanced aggregates can be designed in the future. Further, if these peptides can also exhibit highly specific biomolecule recognition, fibrils can be designed to both recognize their target molecule, and to carry out chemical reactions on that target molecule.

The use of such a simple system to produce efficient protein-like functions provides a powerful tool for biomaterial design. Their simplicity makes them easy to produce, while their display of synergistic activity affords virtually limitless possibilities of functionality. Furthermore, this work provides insight into how life's first proteins may have evolved.

Table of Contents

Acknowledgements

First, I'd like to thank my parents, who from a young age encouraged my interest in science and pushed me to excel at my academic studies. Without their support I would not be anywhere near the student that I am today.

I'd also like to thank Caroline Rufo, who was the graduate student that took me under her wing 3 and a half years ago, when I first joined the Korendovych lab. Her training was invaluable and has led to my abilities as an independent researcher in the lab. I would like to thank Alex Sternisha, for his help in the lab, particularly on the biomolecule recognition project. I would also like to extend my thanks to the entire Korendovych lab, for providing support, advice, and a friendly lab environment to spend my 4 years at Syracuse in.

A great appreciation goes to Dr. Ivan V. Korendovych, who accepted me into his lab at the end of my freshman year. He has been a tremendous mentor, keeping me on track to stay competitive and succeed during my undergraduate career. He has always pushed me to be one step ahead of where I am currently, and has greatly aided in my development as a scientist.

Finally, I'd like to thank the Renee Crown Honors Program, for providing me with many unique opportunities during my undergraduate career, including the development of this Capstone project. They have also providing funding through a Crown Award for a portion of my Capstone project.

Introduction

Proteins exhibit a wide variety of extremely efficient functions. Antibodies use highly specific binding interactions to recognize a target molecule, often able to differentiate between differences in a single bond at the binding site. Enzymes can not only display this specificity as well, but also carry out catalysis on the bound target. Replicating such efficiency with *de novo* designed proteins capable of novel functions is one of the Holy Grails of biochemistry. Such unnatural functionality would provide a gateway to new highly efficient biomaterials and catalysts. Attempts to design *de novo* proteins have only shown moderate success, and we are still unable to rival the extraordinary efficiency of those found in nature[1]. New approaches are needed in order to achieve efficient design of novel functionality.

We can gain valuable insights into new minimalistic design techniques by observing how life's first proteins evolved. Underlying a protein's functionality is the ability to fold into a unique stable three-dimensional structure. A typical protein chain consists of at least 100 amino acid residues. This length produces virtually infinite numbers of possible permutations, and it is uncertain how nature could effectively test such massive numbers of possibilities randomly. However, much shorter peptides can also possess well-defined secondary conformations through the formation of amyloid fibrils. One hypothesis regarding protein evolution states that the first proteins arose from similar simple amyloid-forming peptides[2,3]. These peptides could organize into well-defined secondary structures capable of protein-like functions. In the lab, short heptapeptides that alternate hydrophobic residues have demonstrated the ability to form prion-like β-sheet aggregates[4,5,6]. These stable aggregates could serve as a scaffold to introduce functional residues into.

Using minimalistic techniques, simple seven residue peptides capable of self-assembling and carrying out protein-like functions were successfully designed. By inserting polar residues into an alternating hydrophobic peptide backbone, stable aggregates were engineered for specific desired capabilities, including catalysis and biomolecule recognition.

The first series of peptides were designed to self-assemble in the presence of Zn^{2+} (Fig.1). Fibrils capable of zinc-dependent esterase activity were created by introducing histidine residues (a common residue found at zinc-binding sites in metalloproteins) into the alternating hydrophobic core. The Zn^{2+} served to promote both β-sheet-rich fibril formation and hydrolysis of *para*-nitrophenyl acetate (pNPA). We investigated the design, metal-binding interactions, and catalytic properties of these Zn^{2+}-dependent self-assembling fibrils. Furthermore, upon

Figure 1. Self-assembling aggregates can be engineered to carry out enzyme-like catalysis.

mixing peptides of different sequences, synergistic activity was observed, forming fibrils of increased catalytic efficiency. The ability to mix various peptides into a single fibril provides virtually limitless possibilities for the arrangement and structure of functional sites. These short self-assembling functional peptides are the first of their kind. Enzyme-like catalysis from such a simple seven-residue system is unprecedented and provides a powerful platform from which more elaborate and advanced aggregates can be designed in the future.

To further test the use of self-assembling peptides as a potent platform for the design of novel functionality, we designed a series of peptides capable of biomolecule recognition. Our model target molecule is melittin, a cationic α-helical peptide found in bee venom. Its stable secondary structure and both hydrophobic and charged regions provide an ideal target candidate. Peptides
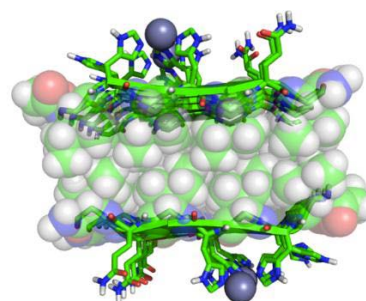
capable of self-assembling, independent of zinc, were first designed. Negatively-charged residues were inserted into the alternating hydrophilic/hydrophobic peptide sequence. These negatively-charged residues target melittin's regions of positive charge. Fibrils capable of binding to melittin were successfully created. Efforts are currently underway to improve the specificity of the fibrils. By mixing peptides, large libraries of fibrils with differing functional sites can be generated. Through high-throughput screening of these libraries for target molecule binding, improved specificity should be attained. The design of these fibrils will demonstrate the ability of functional aggregates to not only carry out novel catalysis, as previously demonstrated, but to exhibit remarkable specificity despite their simplicity.

We have successfully used minimalistic design techniques to create short seven-residue peptides capable of self-assembling into functional aggregates. The first of their kind, these aggregates display protein-like characteristics, providing a powerful tool for biomaterial design. Their simplicity makes them easy to produce, while their display of synergistic activity affords virtually limitless possibilities of functionality. Furthermore, this work provides insight into how life's first proteins may have evolved. Herein we investigate and characterize the properties and capabilities of such peptides.

Chapter One:

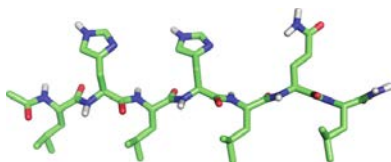*Design of Self-Assembling Peptides for*

Catalysis

1.1 Design of the Peptide Library

To design our initial peptide library we utilized a simple three-step design process. Step one: create an alternating hydrophobic core. Step two: create a metal coordination sphere. Step three: create a secondary coordination sphere (*Figure 1.1*).


```
XXXXXXX    Step 1: create hydrophobic core
LXLXLXL    Step 2: create a metal coordination sphere
LHLHLXL    Step 3: Add polar residues for additional β-sheet/ secondary
LHLHLRL    coordination sphere
LHLHLDL
LHLHLEL
LHLHLYL
LHLHLHL
LHLHLKL
```

Figure 1.1. Design scheme for short self-assembling peptides.

Short heptapeptides that alternate hydrophobic residues have demonstrated the ability to form prion-like β-sheet aggregates[4,5,6]. Step one is to create a core of alternating hydrophobic residues as the scaffold for our functional aggregates. At positions 1, 3, 5, and 7 leucine, a nonpolar residue with a propensity to form β-sheets, was inserted. This hydrophobic core will drive β-sheet and fibril formation, while tolerating considerable variation at positions 2, 4, and 6.

Step two is to introduce a metal coordination sphere. In both natural and artificial enzymes a histidine triad is a common metal-binding motif[7,8,9]. We introduced histidine residues at

positions 2 and 4, in order to form this motif between neighboring β-strands. The histidine triad will coordinate to Zn^{2+}, while leaving an open coordination site for a water molecule, the nucleophile in the esterase reaction.

Step three is to form a secondary coordination sphere at position 6. At position 6 a variety of polar amino acids were inserted and screened for catalytic activity. An initial library of seven peptides was synthesized through Fmoc solid-phase peptide synthesis (*Figure 1.2*).

Figure 1.2. List of initial leucine core peptides. Red residues are the alternating hydrophobic core, blue the metal-binding residues, and gold the hyrdrophilic secondary coordination sphere residues. All peptides were synthesized through Fmoc solid phase synthesis.

Peptide	Sequence
1	Ac-LHLHLDL-CONH$_2$
2	Ac-LHLHLEL-CONH$_2$
3	Ac-LHLHLQL-CONH$_2$
4	Ac-LHLHLYL-CONH$_2$
5	Ac-LHLHLHL-CONH$_2$
6	Ac-LHLHLKL-CONH$_2$
7	Ac-LHLHLRL-CONH$_2$

1.2 Screening of Initial Leucine Core Peptides for Catalytic Activity

1.2.1   Michaelis-Menten Kinetics

Enzymes have been shown to follow the Michaelis-Menten model of kinetics. In this model an enzyme (E) reacts with a substrate (S) to form the enzyme-substrate complex (ES). This is the rate-limiting step of the reaction. Once the complex is formed, the substrate is rapidly converted to and released as product (P), resulting once again in free enzyme. This reaction scheme is demonstrated by the following equation (*Figure 1.3).*

$E\ +\ S\ \rightleftarrows\ ES\ \rightarrow\ E\ +\ P$ (***Figure 1.3***)
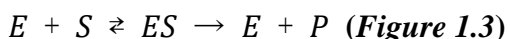
By relating the rate of the reaction to substrate concentration, figure 1.3 can be used to derive the Michaelis-Menten equation (*Figure 1.4*).

$$V_0 = (k_{cat}[E][S])/ (K_M + [S])$$ ***Figure 1.4***

According to this model, the appearance of product is linear to the substrate concentration until the enzyme binding sites become saturated and the rate levels off (known as V_{max}). k_{cat}, a measure of turnover number, and K_M, a measure of how tightly the enzyme binds the substrate, can be used to calculate k_{cat}/K_M (a commonly used measure of catalytic efficiency).

1.2.2 Choosing pNPA As A Benchmark Reaction

In order to evaluate the catalytic efficiency of our fibrils, a benchmark reaction is needed. In the literature, many zinc-binding metalloenzymes are assayed by the hydrolysis of *para*-nitrophenyl acetate (pNPA) (*Figure 1.5*)[10,11].
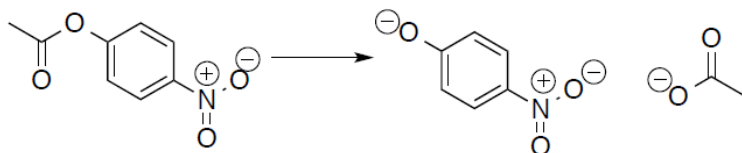

Figure 1.5 *The hydrolysis of pNPA.*

This allows for easy comparison between our fibrils and other previously designed artificial enzymes. The product is yellow-colored with an absorption maxima at 405nm, allowing for the rate of reaction to be easily monitored in a 96-well platereader.

1.2.3 Catalytic Activity of Leucine-Core Peptides

14

The seven leucine-core peptides from Figure 1.2 were assayed using pNPA in the presence of zinc. The results are included in Figure 1.6. They follow the Michaelis-Menten model, indicating enzyme-like activity. The amino acid present at position 6 has a critical role in the catalytic efficiency of the peptide. The catalytic fibrils are extremely sensitive to even single residue changes in the primary amino acid sequence.

Peptide	Sequence	k_{cat}/K_M, $M^{-1}s^{-1}$	k_{cat} x 10^{-2}, s^{-1}	K_M, mM
1	Ac-LHLHLDL-CONH$_2$	0.2 ± 0.1	-	-
2	Ac-LHLHLEL-CONH$_2$	< 0.2	-	-
3	Ac-LHLHLQL-CONH$_2$	30 ± 3	-	-
4	Ac-LHLHLYL-CONH$_2$	13 ± 5	-	-
5	Ac-LHLHLHL-CONH$_2$	0.60 ± 0.08	-	-
6	Ac-LHLHLKL-CONH$_2$	12 ± 2	-	-
7	Ac-LHLHLRL-CONH$_2$	18 ± 4	3.2 ± 0.4	1.8 ± 0.4

Figure 1.6. Results of pNPA assays for the seven leucine-core peptides. All experiments were carried out in 25mM TRIS pH 8 buffer with 1mM ZnCl$_2$. Concentrations of pNPA varied from 0.195, to 0.375, to 0.57, and to 0.75mM.

Peptide 3 displayed the highest activity (k_{cat}/K_M=30 $M^{-1}s^{-1}$), whereas peptides 1, 2, and 5 showed almost no activity. Peptides 4, 6, and 7 all displayed activities that were between these ranges. By changing just a single amino acid at a single position, the activity of the peptides can be tuned to a desired level.

1.3 Establishing Structure-Activity Relationships

Next we sought to develop structure-activity relationships for our peptide catalysts (Figure 1.7). First, we examined the effect of changes to the hydrophobic core of peptide 7. Alanine,

a much smaller and less hydrophobic residue than leucine, resulted in an almost complete loss in activity. In contrast, isoleucine and valine both resulted in similar increases in activity. Both isoleucine and valine are β-branched amino acids and are known to have a higher propensity for β-sheet formation than leucine.

Peptide	Sequence	k_{cat}/K_M ($M^{-1}s^{-1}$)
Position 6 variants		
1	Ac-LHLHLDL-CONH$_2$	0.2 ± 0.1
2	Ac-LHLHLEL-CONH$_2$	<0.2
3	Ac-LHLHLQL-CONH$_2$	30 ± 3
4	Ac-LHLHLYL-CONH$_2$	13 ± 5
5	Ac-LHLHLHL-CONH$_2$	0.6 ± 0.08
6	Ac-LHLHLKL-CONH$_2$	12 ± 2
7	Ac-LHLHLRL-CONH$_2$	18 ± 4
Leucine Substitutions		
7	Ac-LHLHLRL-CONH$_2$	18 ± 4
8	Ac-AHAHARA-CONH$_2$	0.12 ± 0.8
9	Ac-IHIHIRI-CONH$_2$	22 ± 8
10	Ac-VHVHVRV-CONH$_2$	26 ± 4
Combined Substitutions		
11	Ac-IHIHIQI-CONH$_2$	62 ± 2
11a	Ac-VHVHVQV-CONH$_2$	32 ± 2
Primary Ligand Variants		
12	Ac-IAIHIRI-CONH$_2$	0.36 ± 0.16
13	Ac-IHIAIRI-CONH$_2$	0.2 ± 0.4
Removal of N, C-Terminal Blocking Groups		
14	H$_2$N-IHIHIQI-COOH	1 ± 3

Figure 1.7 *Structure-activity relationships of the peptide catalysts. All reactions were carried out at pH 8 in the presence of 1mM Zn^{2+}.*

Next, we combined the substitution to the hydrophobic core with the substitution of glutamine at position 6. The combination of these two substitutions resulted in a doubling of activity in the valine variant and a more than tripling of activity in the isoleucine variant. The most active peptide, peptide 11, displayed a k_{cat}/K_M of $62 \pm M^{-1}s^{-1}$.

In order to probe the importance of the histidines to the coordination of zinc and activity of the peptides, variants with histidine missing at either position 2 or 4 were synthesized. Removing the histidine at either position kills the activity of the peptide, suggesting that both histidines are needed and play a critical role in the catalytic activity of the peptides.

Finally, the N-terminal acyl and C-terminal amino caps were removed from the most active species, peptide 11. This resulted in almost no catalytic activity. This could be due to the introduction of charges to the N- and C-termini. The resulting charges could cause unfavorable electrostatic interactions or disrupt proper β-sheet formation.

1.4 Structural Characterization of Catalytic Peptides

In order to understand the structure of the peptide catalysts, several techniques were utilized. Not only do these techniques reveal extended β-sheets, but also fibril aggregates on the scale of hundreds of nanometers. When compared to the catalytic efficiency of the peptides, several trends between secondary structure and catalytic efficiency are also observed.

1.4.1   Circular Dichroism Spectroscopy

Circular dichroism (CD) measures the angle of rotation of plane-polarized light after it has passed through a chiral sample. Peptides, being composed of chiral amino acids, give off CD signals. The different possible secondary structures give unique and distinguishable signatures, allowing CD to determine the secondary structure present in a given sample (Figure 1.8).
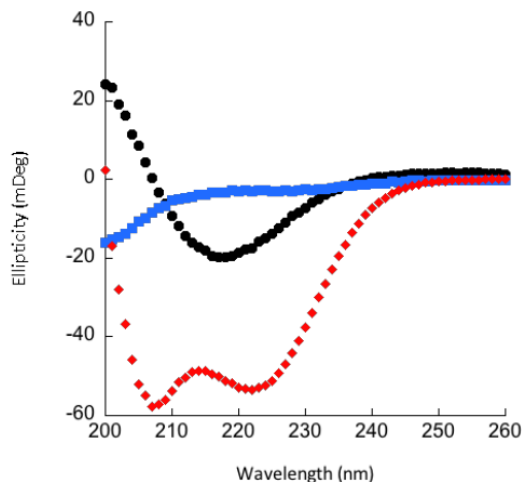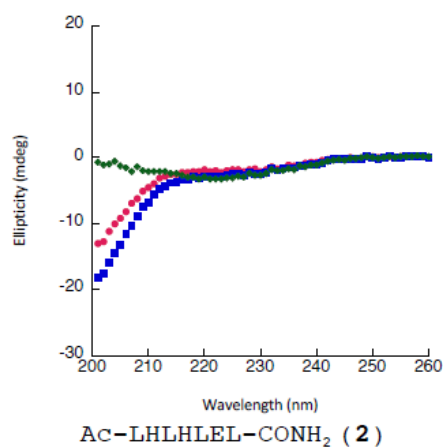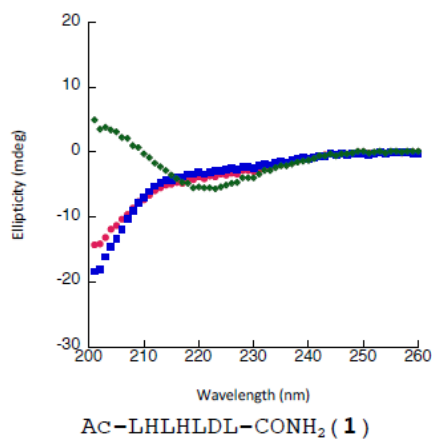
Figure 1.8. *A representative spectral trace of the most commonly observed protein secondary structures. Red represents an α-helix, black a β-sheet, and blue a random coil.*

All of the leucine core peptides in the initial library display a random coil at pH 2 in the absence of Zn^{2+}. This is most likely due to the protonation of the histidine residues at pH 2, preventing the coordination of Zn^{2+}. At pH 8 in the presence of Zn^{2+} all of the leucine core peptides display β-sheet structure. Interestingly, peptides 1, 2, 3, and 6 display no β-sheet structure at pH 8 in the absence of Zn^{2+}, while peptides 4 and 5 do show such structure under these conditions (Figure 1.9). This indicates that β-sheet formation is not solely reliant on coordination to zinc ions, but also on the amino acid present at position 6.
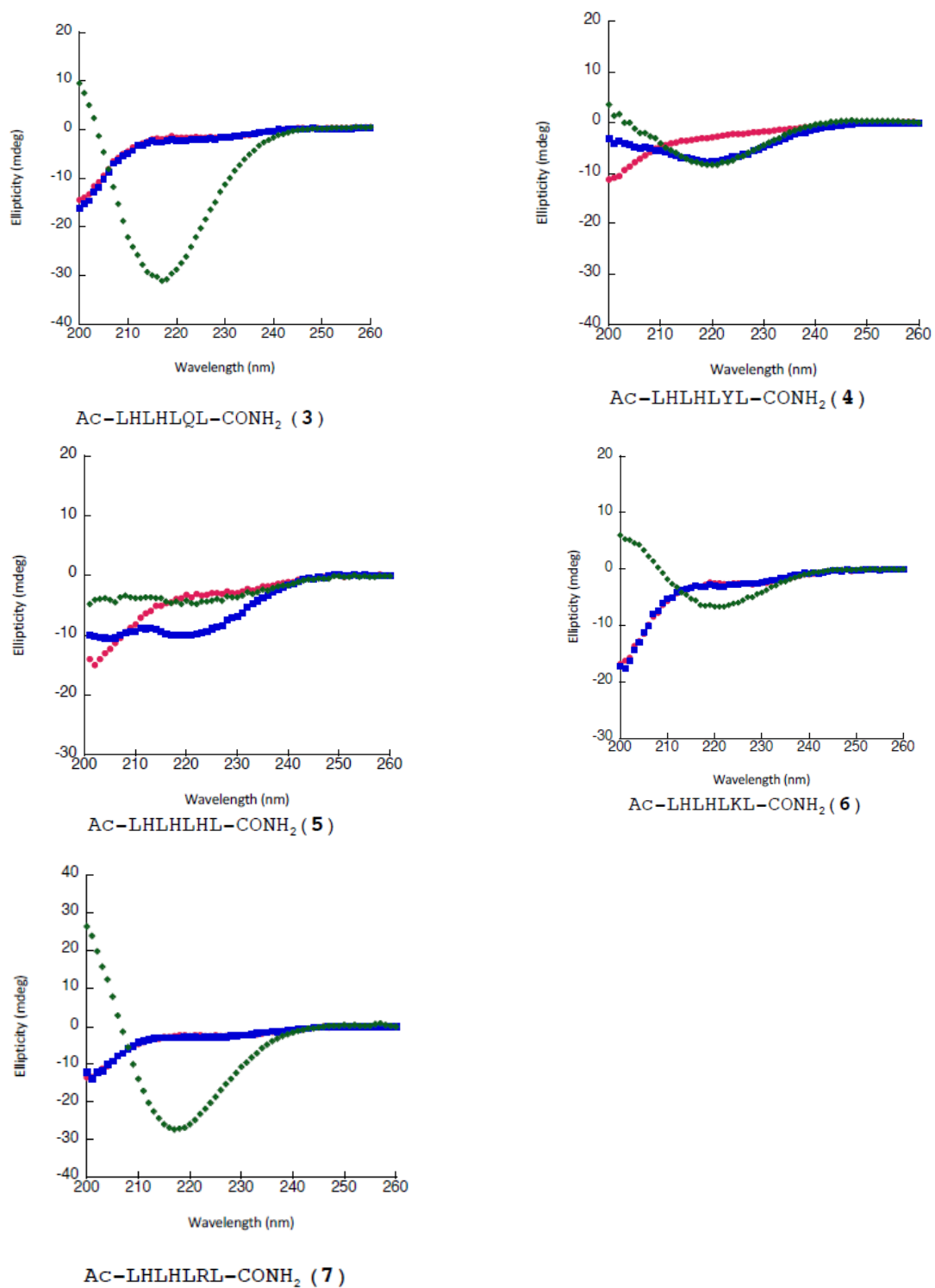

Ac–LHLHLDL–CONH$_2$ (**1**)

Ac–LHLHLEL–CONH$_2$ (**2**)

Ac–LHLHLQL–CONH₂ (3)

Ac–LHLHLYL–CONH₂ (4)

Ac–LHLHLHL–CONH₂ (5)

Ac–LHLHLKL–CONH₂ (6)

Ac–LHLHLRL–CONH₂ (7)

Figure 1.9. Circular dichroism (CD) spectra of designed peptides 1-7. A peptide

concentration of 24µM was used for all experiments. Red circles represent 10mM HCl

The isoleucine variants, which displayed higher activity, also exhibited significantly stronger β-sheet signals in their CD spectra (Figure 1.10). Similar to peptides 1-7, β-sheet formation is absent at pH 2. However, the isoleucine variants display β-sheet formation at pH 8 in both the presence and absence of zinc. This may indicate that the leucine to isoleucine substitution promotes more defined β-sheet structure, and in turn leads to more catalytically active species. Supporting this is peptide 14, the uncapped isoleucine variant, which shows very little β-sheet formation and exhibited very poor catalytic activity.
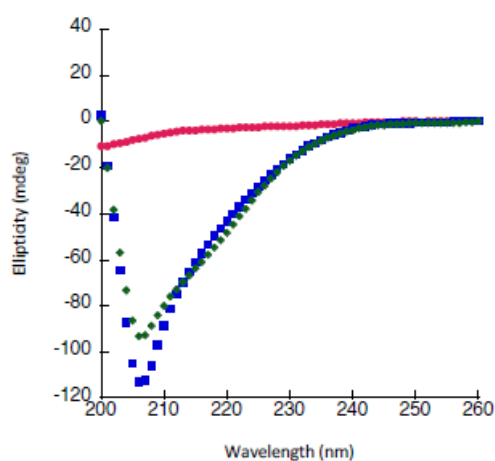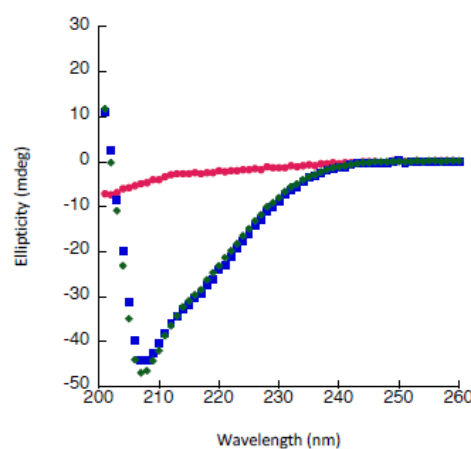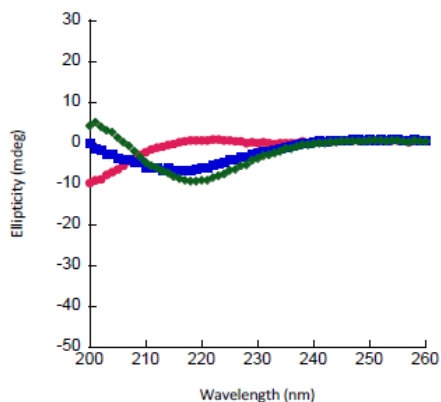

Ac-IHIHIRI-CONH₂ (**9**)
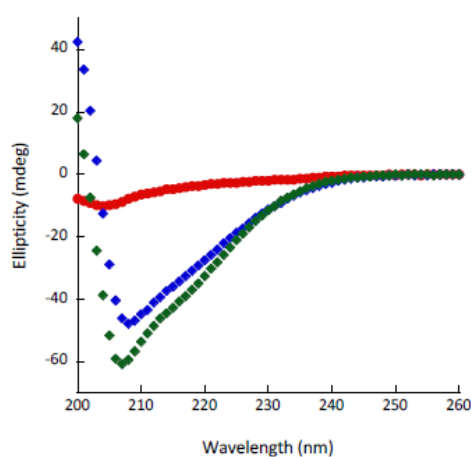
Ac-IHIHIQI-CONH₂ (**11**)
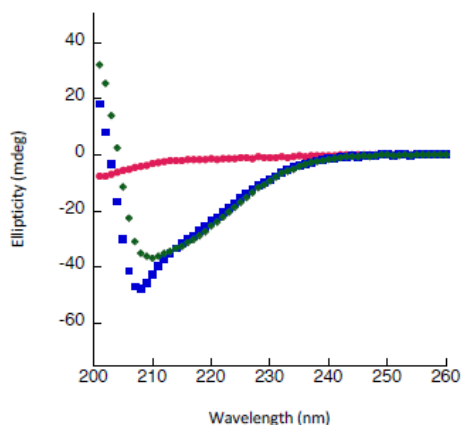

Ac-IAIHIRI-CONH₂ (**12**)
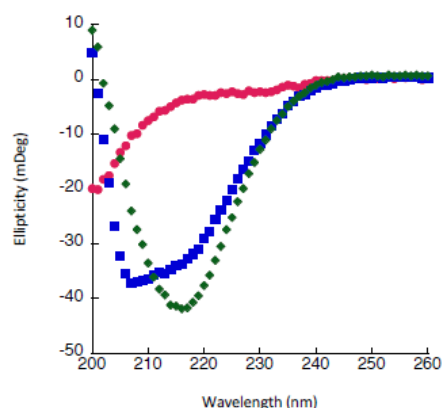

Ac-IHIAIRI-CONH₂ (**13**)

H₂N-IHIHIQI-COOH **(14)**

Figure 1.10. Circular dichroism (CD) spectra of the designed isoleucine variants. A peptide concentration of 25µM was used for all experiments. Red circles represent 10mM HCl pH2, blue squares represent 5mM TRIS pH8, and green diamonds represent 5mM TRIS pH 8 in the presence of 0.5mM ZnCl₂. A 1cm cuvette was used for all CD experiments.

The valine-substituted peptides show a similar trend (Figure 1.11). With the exception of peptide 10, the valine peptides also form β-sheet structures at pH 8 in both the absence and presence of zinc. This also once again corresponds to their higher activity than their leucine variants.
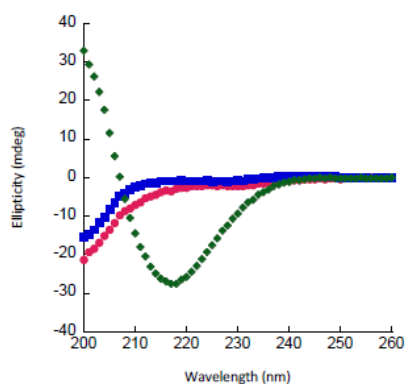
Ac-VHVHVRV-CONH₂ **(10)**

Ac-VHVHVQV-CONH₂ **(11a)**

Figure 1.11. *Circular dichroism (CD) spectra of the designed valine variants. A peptide concentration of 25μM was used for all experiments. Red circles represent 10mM HCl pH2, blue squares represent 5mM TRIS pH8, and green diamonds represent 5mM TRIS pH 8 in the presence of 0.5mM ZnCl₂. A 1cm cuvette was used for all CD experiments.*

Finally, under no tested conditions did the alanine variant (peptide 8) display β-sheet structure (Figure 1.12). This peptide also displayed no catalytic activity.
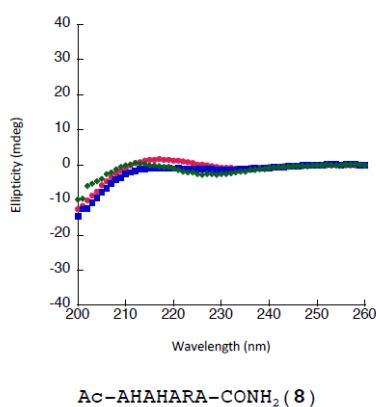

Ac-AHAHARA-CONH₂ (**8**)

Figure 1.12. *Circular dichroism (CD) spectra of the designed alanine variant. A peptide concentration of 25μM was used for all experiments. Red circles represent 10mM HCl pH2, blue squares represent 5mM TRIS pH8, and green diamonds represent 5mM TRIS pH 8 in the presence of 0.5mM ZnCl₂. A 1cm cuvette was used for all CD experiments.*

Based on these CD experiments it appears that catalytic activity is not only correlated to, but dependent on β-sheet formation. The more catalytically active valine and isoleucine variants also show much stronger β-sheet CD signals, even in the absence of zinc. Conversely, peptides such as the alanine variant (8) or the uncapped variant(14), which show little to no catalytic activity, also show either very weak or no β-sheet signal under any of the tested conditions.

1.4.2   Thioflavin-T Binding Assays

β-sheet forming peptides are known to have a propensity to form stable amyloid structures[12.13]. A common technique to detect amyloid structure employs the use of the dye thioflavin-T (Figure 1.13). Upon binding to amyloid aggregates, the fluorescence properties of the dye change, causing an increase in fluorescence that corresponds to the degree of amyloid formation[13-15].
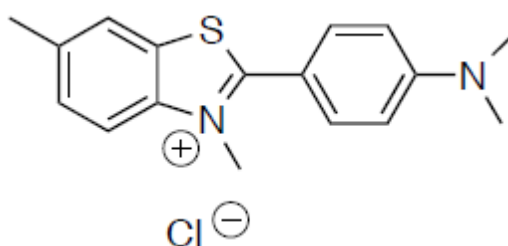

Figure 1.13. *Chemical structure of thioflavin-T.*

Figure 1.14 displays the varying degrees of amyloid formation by the designed leucine-core peptides. The peptides display varying degrees of β-sheet formation, with peptide 4 giving the strongest signal at pH 8.
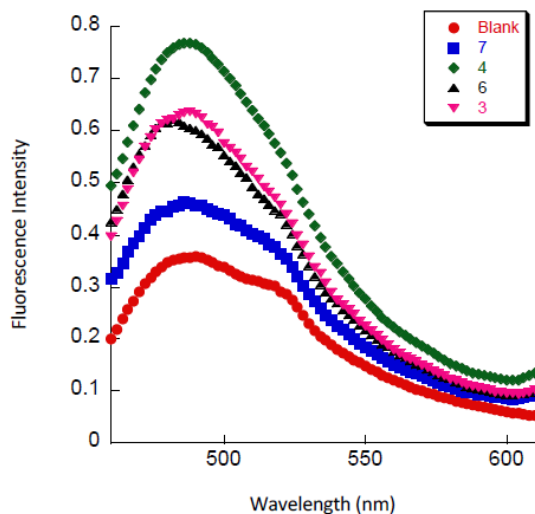
Figure 1.14. *Fluorescence spectrum of thioflavin-T (ThT) in the presence of the leucine-core peptides. Peptide samples were prepared in 25mM TRIS pH 8 with 1mM ZnCl₂. A peptide concentration of 200μM was used.*

Similarly, peptides 9 and 11 of the isoleucine variants also displayed significant amyloid structure (Figure 1.15). Peptides 12 and 13, while they showed β-sheet structure in the CD experiments, did not exhibit significant fluorescence above the blank. These peptides also were not catalytically active. This suggests that while the histidines in positions 2 and 4 are not required for β-sheet formation, they play an important role in both catalytic activity and amyloid aggregation.

Figure 1.15. *Fluorescence spectrum of thioflavin-T (ThT) in the presence of the isoleucine-core peptides. Peptide samples were prepared in 25mM TRIS pH 8 with 1mM ZnCl₂. A peptide concentration of 200μM was used.*

Peptides 10 and 11a, the valine variants, also show fluorescence above the blank (Figure 1.16).

Figure 1.16. *Fluorescence spectrum of thioflavin-T (ThT) in the presence of the valine-core peptides. Peptide samples were prepared in 25mM TRIS pH 8 with 1mM ZnCl$_2$. A peptide concentration of 200μM was used.*

Finally, peptide 8, the alanine variant, shows essentially no fluorescence above the blank (Figure 1.17). Based on these results, it appears that not only is β-sheet formation necessary for catalytic activity, but amyloid aggregation as well. The isoleucine, leucine, and valine-core peptides all show significant amyloid-forming propensity, with the exception of peptides 12, 13, and 14, which all also show little to no catalytic activity.
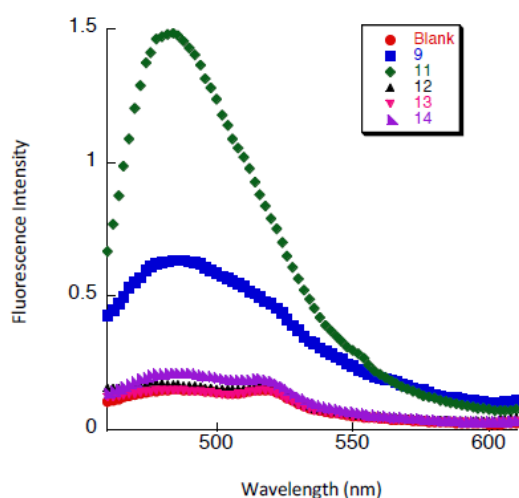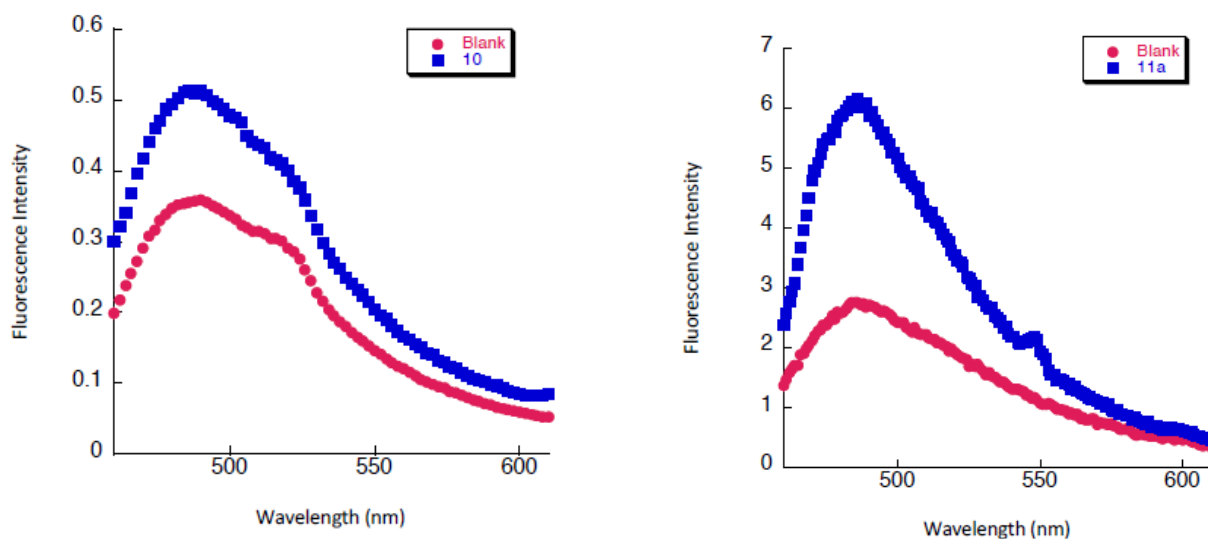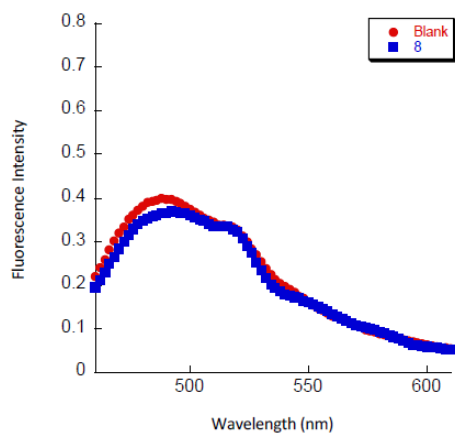
Figure 1.17. *Fluorescence spectrum of thioflavin-T (ThT) in the presence of the alanine-core peptide. Peptide samples were prepared in 25mM TRIS pH 8 with 1mM ZnCl$_2$. A peptide concentration of 200µM was used.*

1.4.3   Transmission Electron Microscopy

With the aid of collaborators from the University of California San Francisco (UCSF) we utilized transmission electron microscopy (TEM) to analyze the morphology of the fibrils. In Figure 1.18 two images of peptide 7 are shown. The images, one at 0 hours and the other at 72 hours, show a lag in the formation of mature amyloid fibrils. This is consistent with the common maturation process found in self-aggregating fibrils. Peptide monomers first assemble into small oligomeric protofibrils and then into fully mature fibrils[x]. At 0 hours peptide 7 displays the characteristic protofibrils, but at 72 hours these protofibrils have matured into the full fibrils.
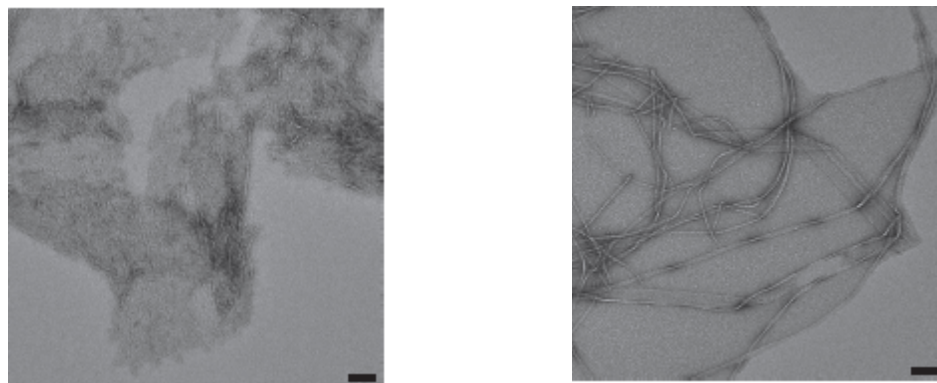

Figure 1.18. (Left) TEM image of peptide 7 at 0 hours. (Right) REM image of peptide 7 at 72 hours. Peptide concentration is 25µM. (25,000x magnification, size bar 100nm).

Interestingly, peptide 11, the isoleucine derivatives, showed much more rapid formation of mature fibrils. Mature fibrils were present at both 0 hours and 72 hours (Figure 1.19).
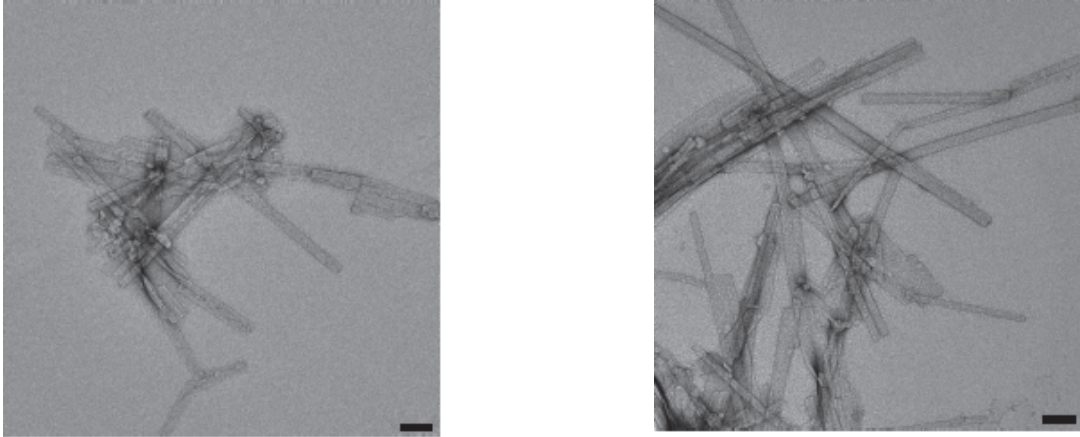
Figure 1.19. (Left) Peptide 11 at 0 hours and (Right) 72 hours. Peptide concentration is 25μM. (25,000x magnification and size bar 100nm.)

This suggests that the characteristics of fibril formation can be tuned through altering the sequence of the hydrophobic core.

1.5 Structural Modelling

Collaborators at UCSF aided us in producing a crude structural model of the amyloid aggregates. The sequence of peptide 11 (IHIHIQI), our most active peptide, was submitted to the zipperdb database and broken up into 6-residue fragments[x]. Rosetta[x] *ab initio* folding generated 100 models of 7-residue peptides. The top result was aligned into the zipperdb template with an acetylated N-terminus and amidated C-terminus. This served as the starting model. The Rosetta relax protocol was used to generate 200 trajectories for under the conditions of zinc coordination. This generated the model shown in Figure 1.20.

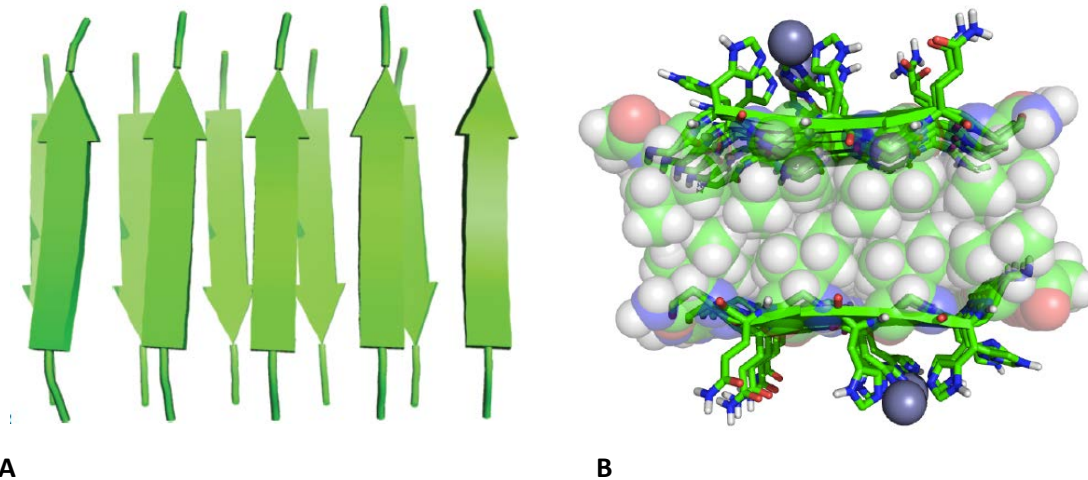*Figure 1.20.* *(A) Structural modelling shows peptide strands in a parallel arrangement within the β-sheet. (B) Structural modelling of the packing of the hyrdrophobic core. Structural modeling done by Xiaozhen Hu, UCSF.*

The model aligns with many of our experimental predictions and conclusions. The strands are arranged in a parallel fashion. Zinc is also bound to three histidines, two from one strand, and a third from the neighboring strand.

1.6 Mixing Peptides for Synergistic Activity

Short 7-residue peptides offer a simple system for designing amyloidogenic catalysts. Even with just 7 residues the number of possible sequences present with a 20 residue library is 1.28×10^9. However, as observed in our studies, only a small fraction of these are capable of amyloid formation and catalysis. By retaining a consistent hydrophobic core and both histidine residues, while varying position 6, this leaves a combination of just 3 different amino acids in a given strand. While this still provides a relatively large number of possibilities, the diversity can be greatly expanded by thinking of active species as a mixture of 2 peptides. Two separate peptides could mix into the same fibril to form functional groups that are a combination of the two strands.

To test whether our peptides are capable of synergistic activity, we mixed two peptides of moderate activity and measured their catalytic activity. Peptides 4 and 7 were mixed in varying ratios. These peptides do not oligomerize at pH 2, so peptide stocks were mixed and then raised to pH 8 with TRIS buffer containing zinc to induce oligomerization. Peptides 4 and 7 did display synergistic activity, with a max catalytic activity at 50% of each peptide (Figure 1.21).
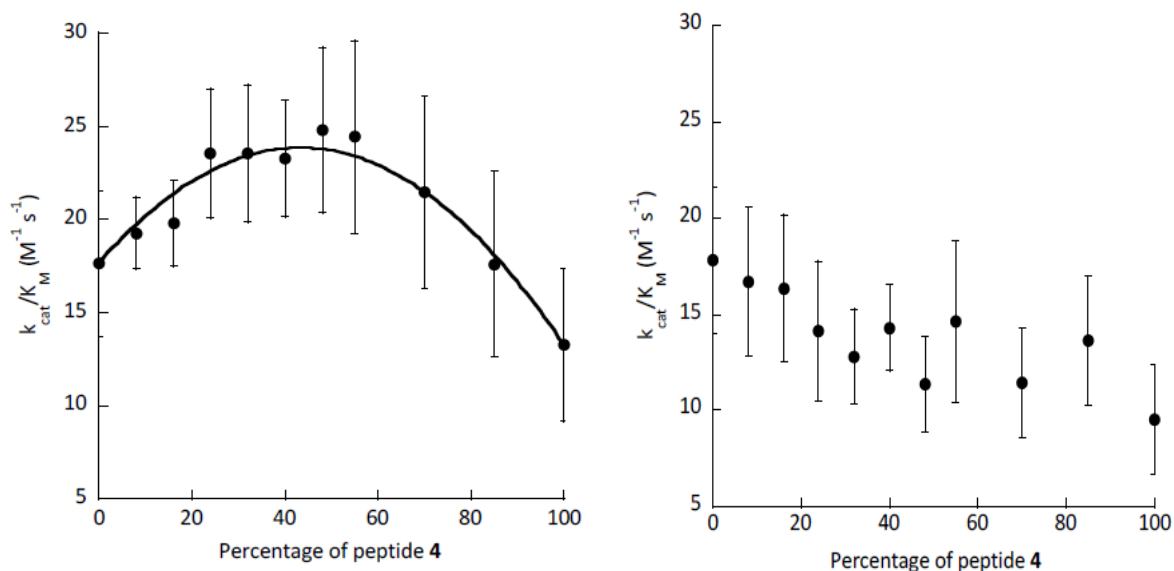
Figure 1.21. The catalytic efficiency of varying ratios of peptide 4 and 7. Graph on left results from mixing peptides before inducing fibril formation. Graph on right results from mixing preformed fibrils.

In contrast, if the peptides are raised to pH 8 and then mixed, no synergistic activity is observed. This may be due to the preformed fibrils being too bulky and stable to mix together well. Peptides at pH 2 have not formed fibrils and can thus adequately mix together before oligomerization is induced.

1.7 Conclusions

Short seven-residue peptides capable of carrying out ester hydrolysis were designed. They follow Michaelis-Menten kinetics and the most active species achieved a kcat/K_M of $62M^{-1}s^{-1}$. Zinc plays a role not only in catalysis, but in the formation of stable secondary structures. The active species form β-sheet rich amyloid fibrils. These stable arrangements are also necessary for catalytic function. By altering the hydrophobic core or a single residue at position 6, the activity of the peptides can be tuned drastically. Finally, these peptides also exhibit synergistic activity upon mixing. This opens the door to virtually limitless possibilities of combinations in a single fibril.

These catalytic aggregates are the first of their kind and offer a novel approach to biomaterial design. Their simplicity makes them easy and cost-effective to produce. Despite this simplicity, they have the potential for remarkable diversity through the use of peptide mixing strategies. These peptides could provide a simple yet highly efficient new strategy for biomaterial design.

Chapter Two:

Design of Self-Assembling Peptides for

Biomolecule Recognition

All work in the following chapter has been performed by the following authors, unless otherwise stated:

Smith, T. A., Sternisha, A., *Korendovych, I. V.

2.1 Design of the Peptide Library

Enzymes not only carry out efficient catalytic activity, but also display high specificity for their target molecule. Antibodies, likewise, identify antigens with extremely high specificity. These proteins can often distinguish between differences in a single bond, preventing promiscuous and unwanted interactions from taking place. To further test the ability of self-assembling peptides to carry out protein-like functions, we aimed to design peptides capable of biomolecule recognition.

Melittin is a 26-residue cationic α-helical antimicrobial peptide with the sequence *GIGAVLKVLTTGLPALISWIKRKRQQ* (Figure 2.1). Found in bee venom, it is thought to disrupt the cell membrane. Melittin makes an ideal target due to its relatively small size and well-defined secondary structure. Melittin also contains regions of positively charged residues and polar residues, offering the possibility of both electrostatic and polar interactions between melittin and the fibrils[16].
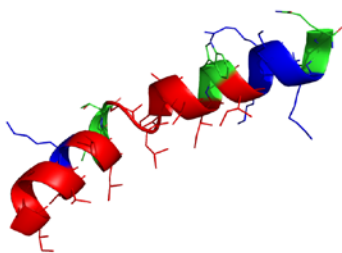
Figure 2.1. 3-dimensional structure of melittin, with side chains exposed. Positively charged regions are highlighted in blue, polar regions in green, and nonpolar regions in red.
Melittin sequence:
GIGAVLKVLTTGLPALISWIKRKRQQ
Structure generated in Pymol with PDB 2MLT

A series of peptides were designed to target melittin (Figure 2.2). In order to facilitate amyloid-formation, an alternating hydrophobic core composed of leucine residues was maintained. In the remaining positions combinations of negatively

32

charged glutamate residues and various polar residues were added. The negative

glutamate residues will target the melittin through electrostatic interactions. The polar

residues may help increase specificity of binding. While polar interactions such as

hydrogen bonding are weaker than electrostatic interactions, they require the two

components to be closer in space, leading to tighter binding between melittin and the

fibrils which more closely can identify its shape. The accumulation of multiple

specific polar interactions may lead to certain fibrils exhibiting specificity for the

target molecule.

Peptide Number	Sequence
BR-1	Ac-LELELQQ-CONH$_2$
BR-2	Ac-LELYLEL-CONH$_2$
BR-3	Ac-LNLELQL-CONH$_2$
BR-4	Ac-LELNLQL-CONH$_2$
BR-5	Ac-LELHLQL-CONH$_2$
BR-6	Ac-LHLELQL-CONH$_2$
BR-7	Ac-LELHLYL-CONH$_2$
BR-8	Ac-LHLELYL-CONH$_2$

Figure 2.2. Designed peptides for binding to melittin. Peptides were acetylated on

the N-terminus and amidated on the C-terminus. All peptides were synthesized by

manual solid-phase synthesis.

2.2 Thioflavin-T Binding Assays

In order to use these peptides as a functional biomaterial, the formation of an

amyloid aggregate is essential. By forming a stable 3-dimensional structure it allows

for the fibrils to display functional groups on the surface which can bind to the target

molecule. The single peptides by themselves in solution would lack the size and

stability necessary to specifically recognize a target. To evaluate the propensity of the

designed peptides to aggregate, we used thioflavin-T assays, as in Chapter 1 (Figure

2.3).
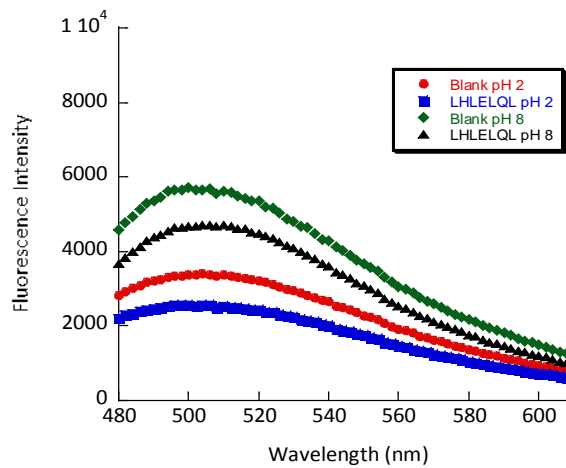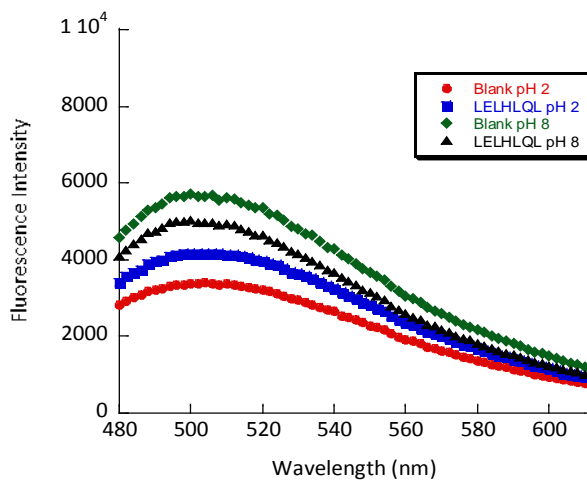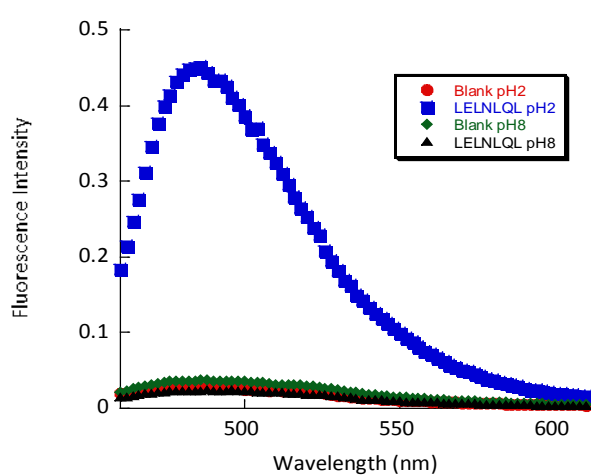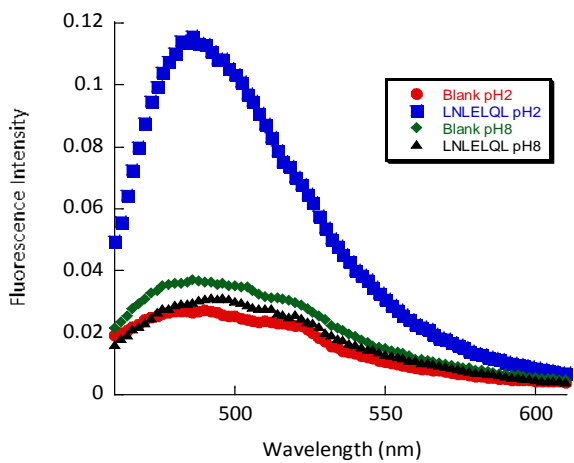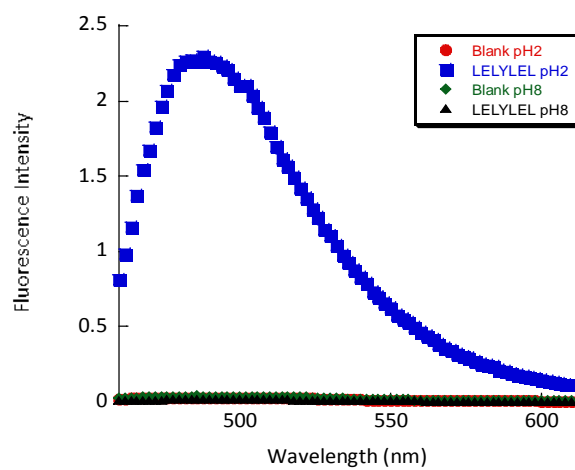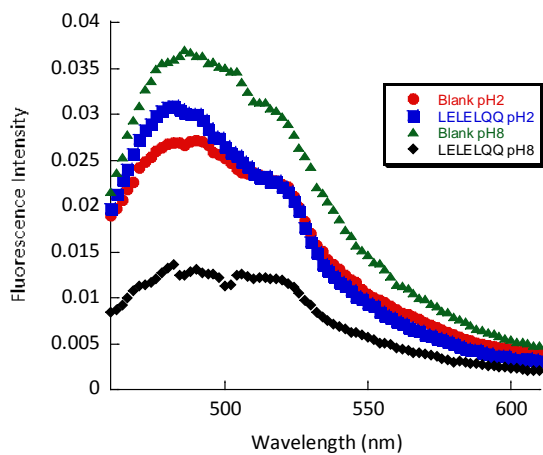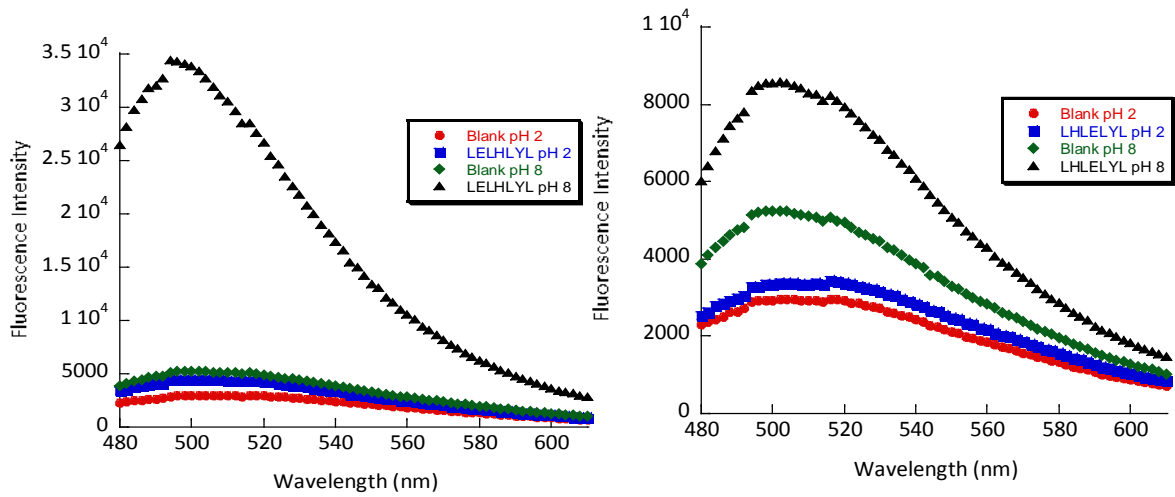
Figure 2.3. Thioflavin-T experiments for peptides BR-1 to BR-8. The blank at pH 2 is represented by a red circle, peptide at pH 2 a blue square, blank at pH 8 a green diamond, and peptide at pH 8 a black triangle.

Interestingly, the majority of the peptides only aggregate at pH 2 and not pH 8. This may be due to the protonation of the glutamate residues at low pH. When deprotonated the residues are charged and may repel each other, preventing aggregation. However, in the case of peptides BR-5 and BR-6, where a histidine is inserted into either position 2 or 4 and a glutamine into position 6, the peptides do not aggregate significantly at either of the two pHs. BR-7 and BR-8 do aggregate at pH 8 and not pH 2. This may be due to the protonation of histidine acting as a molecular switch. At low pH the histidine is protonated and charged, preventing fibril formation. At high pH it deprotonates and is neutral. This may be enough to overcome repulsion by the deprotonated glutamates at pH 8 and allows for aggregation.

For our binding experiments we chose to use peptides BR-7 and BR-8. Amyloids that form under higher pH conditions are desirable not only because the glutamates are deprotonated, allowing for electrostatic interactions, but pH 8 is also much closer to standard biological pH.

2.3 Synthesis of Fluorescently-Labelled Melittin

To test whether our designed fibrils are bound to melittin a fluorescent probe must be added to the melittin peptide. Dr. Yurii Moroz previously synthesized dansyl-lysine, a derivative of lysine that contains a dansyl fluorescent tag on the lysine side chain (Figure 2.4).
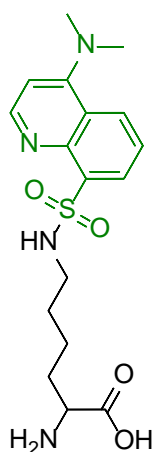
Figure 2.4. The chemical structure of dansyl-lysine.

Dansyl-lysine can easily be added on to the N-terminus of melittin during solid-phase peptide synthesis. Dansyl-lysine is known to have an extinction coefficient of 3,400 $M^{-1}cm^{-1}$ at 330nm when attached to a polypeptide chain. It is an ideal probe for our purposes as it drastically changes its fluorescent properties when its environment is altered[17]. By monitoring shifts in the emission maximum at 540nm (excitation at 330nm) in the presence and absence of fibrils, we can determine if melittin is binding.

2.4 Melittin-Binding Assays

To evaluate binding of the designed peptides to the fluorescently-tagged melittin,

25μM of peptide was mixed with 20μM of melittin at pH 8 using a TRIS buffer. The

solution was excited at 330nm and its fluorescence emission was measured from

480nm to 640nm. All 8 of the initial designed peptides were screened for binding

(Figure 2.5).
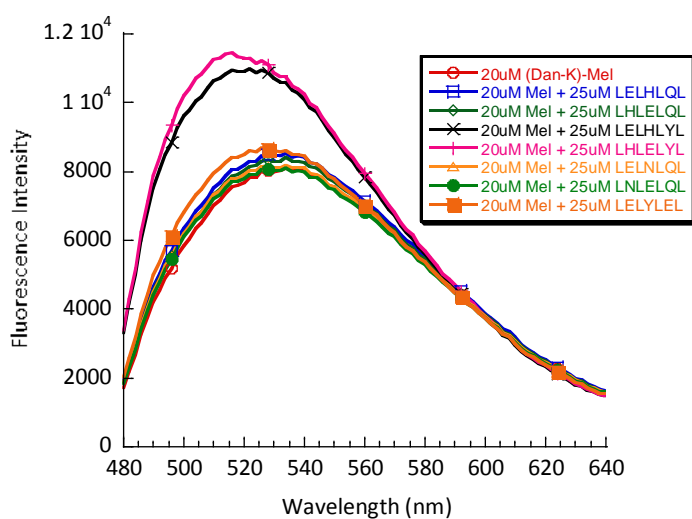
Figure 2.5. *Melittin-binding assays of the 8 designed peptides. Binding is associated with a significant shift in the emission maximum of free melittin*

Of the 8 initial peptides, only BR-7 and BR-8 induce large shifts in the

fluorescence maximum of fluorescently-tagged melittin. A large increase in intensity

is observed along with a blueshift in the location of the maximum. BR-7 and BR-8

are also the only two peptides that form aggregates at pH 8. This indicates that the

formation of amyloid aggregates is essential for binding to the target molecule, and

the single peptide species in solution are not sufficient.

2.5 Testing Specificity of Fibril Binding

To test the specificity of BR-7 and BR-8, binding assays were also done with

fluorescently-tagged magainin I, another cationic antimicrobial agent. Magainin I is a

similar length to melittin and has a sequence of *GIGKFLHSAGKFGKAFVGEIMKS*. The concentration of melittin and magainin was also decreased to 5μM and the concentration of designed peptide was increased to 50μM, in order to reduce non-specific binding. Results of the binding assays are in Figure 2.6.
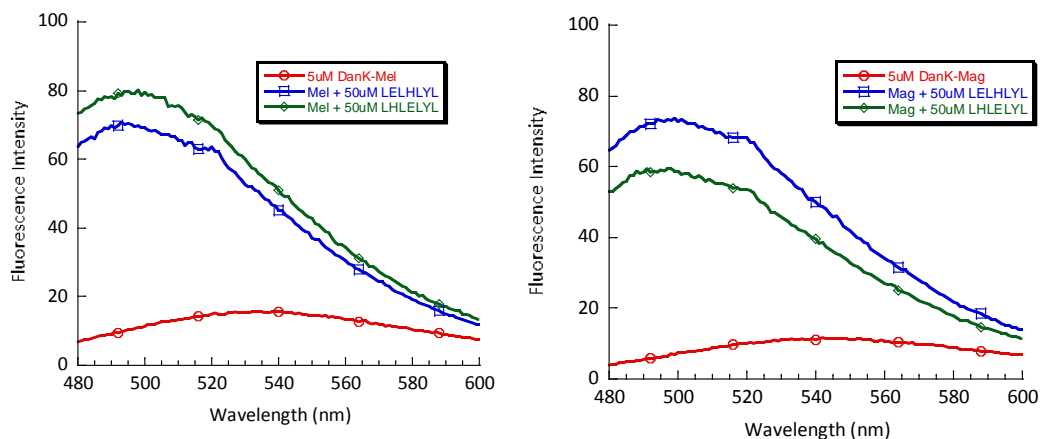
Figure 2.6. Binding assays of 50μM fibrils to 5μM fluorescently-tagged melittin or magainin. Binding assays were carried out at pH 8 in TRIS buffer.

The binding assay reveals that both BR-7 and BR-8 bind to both melittin and magainin with considerable affinity. In order to better understand the binding interactions at work, we next developed a negatively-charged derivative of melittin.

2.6 Probing the Binding Interactions

In order to probe the interactions between the melittin molecule and the fibrils, all of the positively charged residues in melittin were replaced with glutamate residues. This changes the charge of these residues from positive to negative. This "melittin E" molecule exhibited virtually no binding to BR-7 and BR-8, suggesting that binding is highly dependent on electrostatic interactions (Figure 2.7).
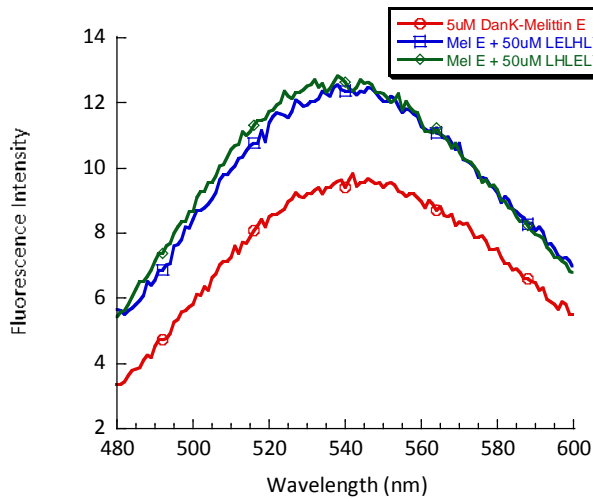
Figure 2.7. *Binding assay of BR-7 and BR-8 to mellitin E. Measurements were taken at pH 8 in TRIS buffer.*

This may mean that insufficient polar interactions are occurring to observe any significant specifity. Binding is dominated by electrostatic interactions in BR-7 and BR-8.

2.7 Ultra-Centrifugation Experiments

Finally, to confirm that it is the large molecular weight species binding to melittin and not small molecular weight species in solution, we did a series of ultra-centrifugation experiments. Fluorescently-labelled melittin was spun at 25,000rpm for 1 hour, both in the presence and absence of fibrils. A fluorescence spectrum was obtained of the solution before ultra-centrifugation, of the supernatant after ultra-centrifugation, and of the solution after the spun-down sample had been resuspended. Results are in Figure 2.8.
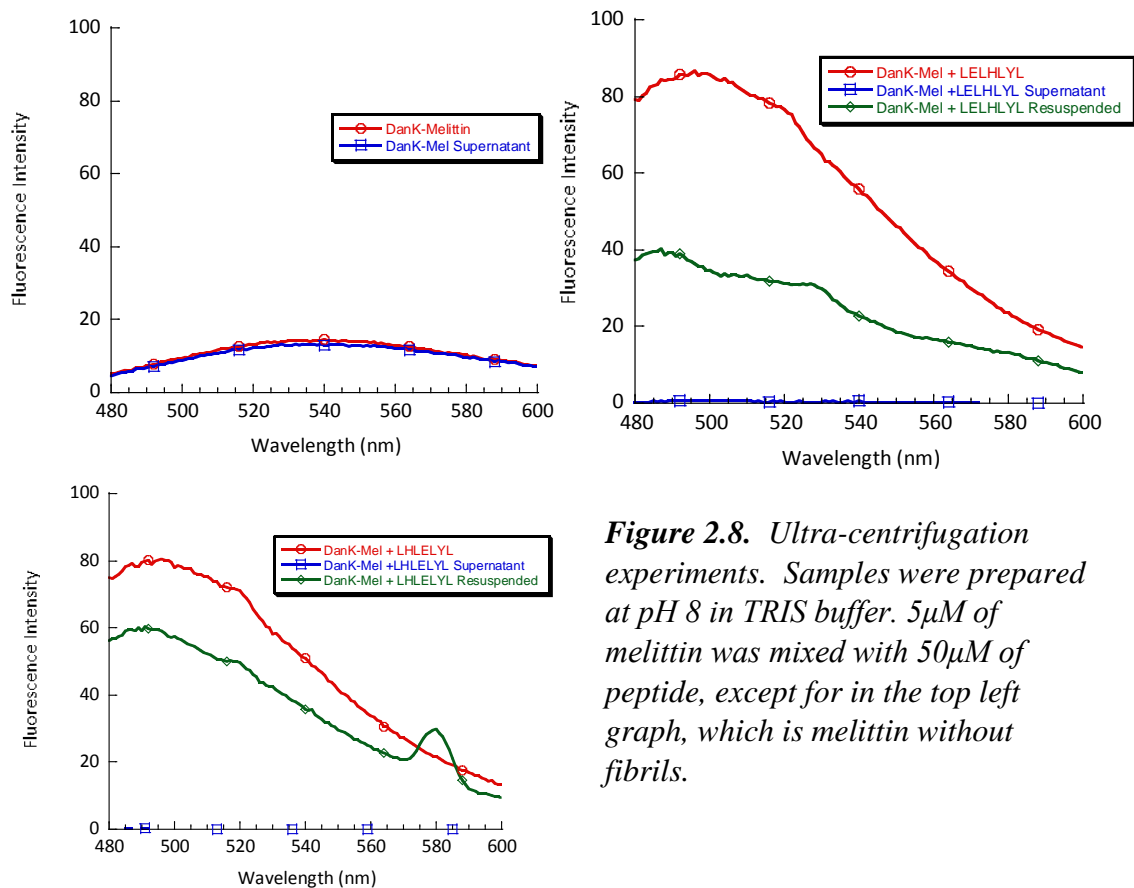
Figure 2.8. *Ultra-centrifugation experiments. Samples were prepared at pH 8 in TRIS buffer. 5µM of melittin was mixed with 50µM of peptide, except for in the top left graph, which is melittin without fibrils.*

As is apparent, melittin does not spin down out of solution by itself. However, in the presence of fibrils BR-7 and BR-8, the fluorescence disappears after ultra-centrifugation. The fluorescence partly returns after the centrifuge sample is mixed and resuspended. The high molecular weight species are binding to the melittin and pulling it out of solution. It is the large fibrils that bind to the target molecule.

2.8 Conclusions

We successfully designed peptides that, upon aggregating into amyloid fibrils, bind to melittin. The formation of fibrils is also necessary for binding. Single peptides dissolved in solution are not sufficient to bind melittin or pull it out of solution. However, the fibrils do not display significant selectivity for melittin over magainin,

another similar cationic antimicrobial peptide. Experiments with a negatively-charged variant of melittin suggest that the binding interactions are dominated by electrostatic interactions. These are relatively strong interactions and may be why there is not much preference for melittin over magainin.

In the future, the specificity of these peptides could be improved through peptide mixing techniques. By incorporating peptides that have a higher propensity for hydrogen bonding, such as LYLYLYL or serine containing peptides, more specific polar interactions could be introduced into the fibril. This could lead to more specific binding and higher recognition of the target molecule. The fibrils also need to be structurally characterized more to determine their secondary structure and morphology.

Peptides capable of specific biomolecule recognition offer a versatile platform for biomaterial design. Fibrils capable of biomolecule recognition could be mixed with catalytic fibrils to create biomaterials that bind a specific substrate and carry out catalysis on it. One application would be in designing a biomaterial to bind and neutralize an environmental toxin. Due to the large size and stability of the fibrils, they can also easily be placed on a filter for mechanization. Self-assembling peptides capable of protein-like functions offer a versatile, simple, and efficient platform for future biomaterial design.

Chapter Three:

Materials & Methods

3.1 Peptide Synthesis & Purification

Peptides were synthesized by manual fluorenylmethyloxycarbonyl (FMOC) solid-phase peptide synthesis under elevated temperature[x]. A reactions were carried out on a 0.1 mmol scale. A ChemImpex Rink Amide Resin was used as a solid support. The resin was swelled in dimethylformamide (DMF) at room temperature for 30 minutes then lowered into a 65°C oil bath. The resin was deprotected for 5 minutes with 5% piperazine and 0.1 hydroxybenzotriazole (HOBt) in DMF. Amino acids were coupled to the resin for 7 minutes using an AA:HCTU:DIPEA:resin (3:2.8:6:2:1 v:v:v) mixture in DMF. Between deprotection and coupling steps the resin was washed 4 times with DMF for 30 seconds each. After the last coupling reaction the peptide is deprotected and raised out of the 65°C oil bath. An acetyl cap is added by coupling the N-terminus with 6 equivalents of acetic anhydride (Ac_2O). Resin was dried under vacuum for approximately 20 minutes. Peptides were cleaved from the resin and side chains were simultaneously removed with a mixture of trifluoroacetic acid (TFA)/H_2O/triisopropyl silane (TIS) (95:2.5:2.5 v:v) for 2 hours at room temperature. The crude peptides were precipitated and washed with cold methyl-*tert*-butyl ether (MtBE). Peptides were purified on a Varian Star 210 preparative reverse phase HPLC system. A Vydac C4 preparative column was used with a linear gradient of solvent A (0.1% TFA in MilliQ H_2O) and solvent B (90% CH_3CN, 10% H_2O, 0.1%TFA). MALDI-TOF mass spectrometry with a Bruker Autoflex III Smartbeam mass spectrometer was used to confirm the identities of the purified peptides. Purity was determined with a Shimadzu Prominence UFLC instrument and an analytical Zorbax Eclipse XDB-C18 column.

3.2 Preparation of Peptide Stocks

Purified peptides were lyophilized to remove solvent. Lyophilized peptides were dissolved in either 10mM hydrochloric acid or trifluoroethanol (TFE) to make a 1mM stock solution. Concentration was determined by absorbance at 214nm as measured by an Agilent 8453 UV-Vis spectrophotometer. Extinction coefficients were calculated using literature values[18]. The pH 2 stock was stable for at least a week.

3.3 Circular Dichroism Spectroscopy

A JASCO J-715 spectrometer was used to collect CD spectra. Data was collected in step-scan mode (4s) and averaged over three runs. Sample was held in a quartz cuvette with a 1cm path length. Peptide concentrations were held at 24μM in either 10mM HCl, 5mM TRIS (pH8), or 5mM TRIS (pH8) with 0.5mM $ZnCl_2$.

3.4 Thioflavin T Assays

ThT assays were carried out on an ATF 105 spectrometer (Aviv Instruments, Inc.) at 25°C. The instrument was operated in the steady-state mode with emission and excitation band pass set to 4nm. Samples were placed in a quartz cuvette with 5mm excitation and 5mm emission pathlengths. Peptide concentration was held at 200μM in either 10mM HCl, 25mM TRIS (pH8), or 25mM TRIS (pH8) with 1mM $ZnCl_2$. ThT was added to a final concentration of 25μM.

3.5 Transmission Electron Microscopy

Peptide stocks were diluted to approximately 25μM in 25mM TRIS (pH8) and 1mM $ZnCl_2$ or $CoCl_2$. 7μL were absorbed for 2-5 minutes onto formvar/carbon-coated, 200-mesh copper grids (Ted Pella, Redding, CA; glow-discharged prior to use). Grids were briefly washed with 0.1 M and 0.01 M ammonium acetate buffer, and stained with two 50μL drops of

freshly filtered 2% (w/v) uranyl acetate. Samples were viewed with a FEI Tecnal F20

electron microscope (FEI Company, Hillsborough, OR) at an acceleration voltage of 80kV.

Electron micrographs were recorded on a Gatan (Pleasanton, CA) UltraScan CCD camera.

3.6 Kinetic Assays

A Thermo Labsystems Multiskan Spectrum plate reader was used to monitor absorbance of

the product (p-nitrophenol) at 405nm and 22°C in 96 well plates. p-Nitrophenylacetate

substrate as diluted to a 0.1M stock in acetonitrile. 150μL of freshly prepared substrate

solution in 25mM TRIS (pH 8), 1mM $ZnCl_2$ was added to 50μL of buffered peptide

stocksolution at pH 8.

3.7 Mixing Experiments

When mixing at pH 8, 135μL of each 1mM stocks of peptides in 10mM HCl were separately

mixed with 15μL of isopropanol and 1.35mL of 25mM TRIS (pH 8) with 1mM $ZnCl_2$.

These solutions were allowed to incubate for 48 hours. The stock solutions were then mixed

in the proportions reported to a final volume of 50μL within the well. To each well was

added 100μL of 25mM TRIS (pH 8) with 1mM $ZnCl_2$. 50μL of substrate solution was added

to a final concentration of 195μM. The activity was measured by the protocol in section 3.6.

When mixing at pH 2 the 1mM stock solutions of each peptide were prepared in 10mM HCl

pH 2. 30μL of isopropanol was added to 270μL of each pH 2 stock solution. The two stocks

were mixed to form 40μL samples at various ratios, as reported. 360μL of 25mM TRIS pH 8

with 1mM $ZnCl_2$ was added to each sample, and allowed to incubate for 48 hours. 50μL of

these samples were added to each well of a 96-well plate. Finally, 150μL of substrate

solution was added to each well to a final concentration of 195μM. The activity was

measured by the protocol in section 3.6.

3.8 Melittin Binding Fluorescence Assays

1μL of 1mM melittin stock in TFE and 10μL of fibril stock were added to 189μL of 25mM TRIS pH 8, giving a final melittin concentration of 5μM and a final fibril concentration of 50μM. The solution was excited at a wavelength of 330nm and the emission spectrum was collected from 480nm to 600nm, with a slit of 5nm. A PMT setting of "medium" was used with a scan control setting of "slow."

3.9 Ultra-Centrifuge Studies

20μL of 1mM melittin stock in TFE and 200μL of fibril stock in TFE were added to 3.78mL of 25mM TRIS pH 8. This solution was centrifuged in a Beckman XL-80 ultracentrifuge for 1 hour at 25,000 rpm and 4°C. Fluorescence spectra were taken as reported in section 3.8 of the solution before centrifugation, after centrifugation, and after centrifugation and resuspension of the samples.

References

(1) Korendovych, I. V. *et al. Current Opinion in Structural Biology* **2014,** *27* (0), 113-121.
(2) Carny, O. *et al. The FASEB Journal* **2005,** *19* (9), 1051-1055.
(3) Greenwald, J. *et al. Journal of Molecular Biology* **2012,** *421* (4–5), 417-426.
(4) West, M. W. *et al. Proceedings of the National Academy of Sciences* **1999,** *96* (20), 11211-11216.
(5) DeGrado, W. F. *et al. Journal of the American Chemical Society* **1985,** *107* (25), 7684-7689.
(6) DeGrado, W. F. *et al. Science* **1989,** *243* (4891), 622-8.
(7) Petrik, I. D. *et al. Current Opinion in Chemical Biology* **2014,** *0*, 67-75.
(8) Spevacek, A. R. *et al. Structure* **2013,** *21* (2), 236-246.
(9) Tebo, A. G. *et al. Current Opinion in Chemical Biology* **2015,** *25*, 65-70.
(10) Belieres, M. *et al. Rsc. Advances* **2015,** *5* (45), 35830-35842.
(11) Kim, M. C. *et al. Chemistry - A European Journal* **2014,** *20* (51), 17019-17024.
(12) Colletier, J. P. *et al. Proceedings Of the National Academy Of Sciences Of the United States Of America* **2011,** *108* (41), 16938-16943.
(13) Biancalana, M. *et al. Biochimica Et Biophysica Acta - Proteins and Proteomics* **2010,** *1804* (7), 1405-1412.
(14) Knowles, T. P. J. *et al. Nat Rev Mol Cell Biol* **2014,** *15* (6), 384-396.
(15) Eisenberg, D. *et al. Cell* **2012,** *148* (6), 1188-1203.
(16) Terwilliger, T. C. *et al. The Journal of Biological Chemistry* **1982,** *257* (11), 6016-6022
(17) Chen, R. F. *Analytical Biochemistry* **1968,** *25,* 412-416.
(18) Kuipers, B. J. H. *J. Argicult. Food Chem.* **2007,** *55*, 5445-5451.